Supporting Information for

A pH-sensitive nanoagent self-assembled from a highly negative-charged phthalocyanine with excellent biosafety for photothermal therapy

Bing-De Zheng, Zhen-Liang Huang, Li-Li Lv, Wen-Liang Lan, Jia-Qian Hu, Xingshu Li, Bi-Yuan Zheng, Mei-Rong Ke*, and Jian-Dong Huang*

College of Chemistry, State Key Laboratory of Photocatalysis on Energy and Environment, Fujian Provincial Key Laboratory of Cancer Metastasis Chemoprevention and Chemotherapy, Fuzhou University, Fuzhou 350116, China.

* Corresponding author. Tel: +86-591-22865513; Fax: +86-591-22866227; E-mail: kemeirong@fzu.edu.cn (M.-R. Ke), jdhuang@fzu.edu.cn (J.-D. Huang)

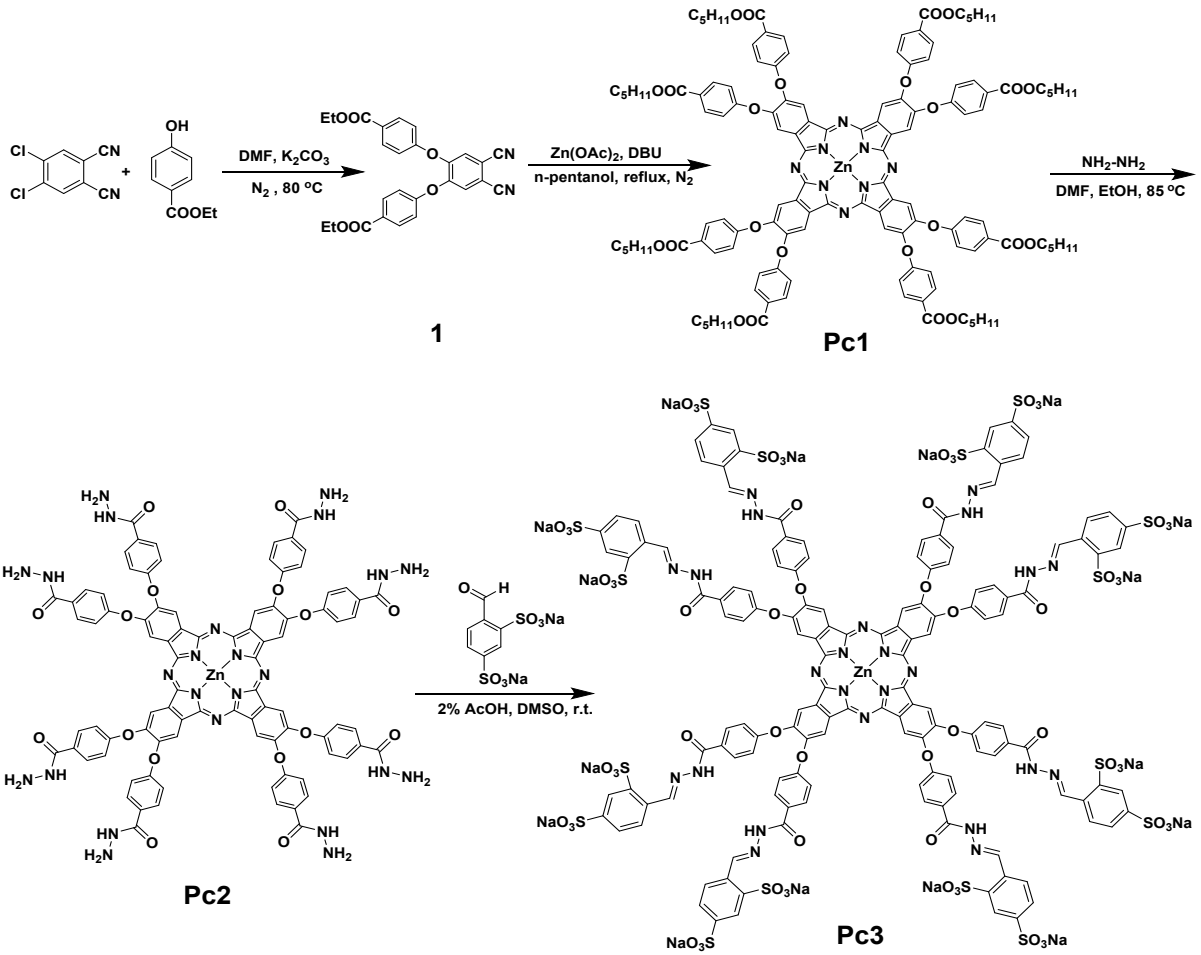

Scheme S1. Synthetic route of **Pc3**.

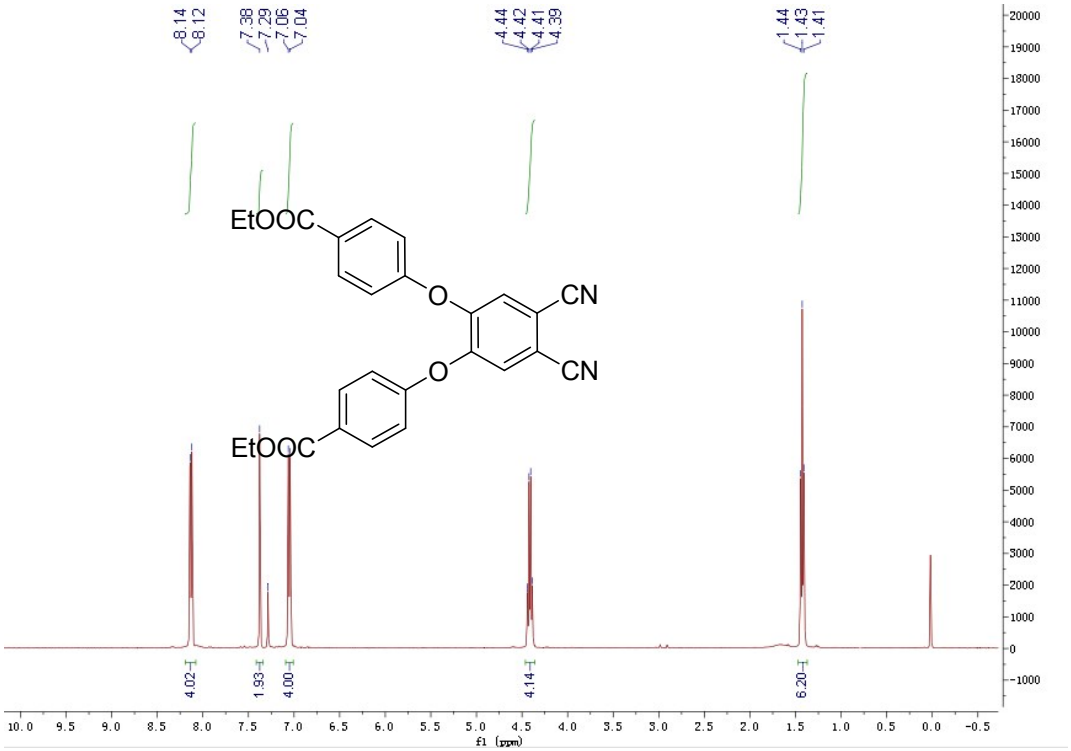

Fig. S1. ^{1}H NMR spectrum of **1** in $CDCl_3$.

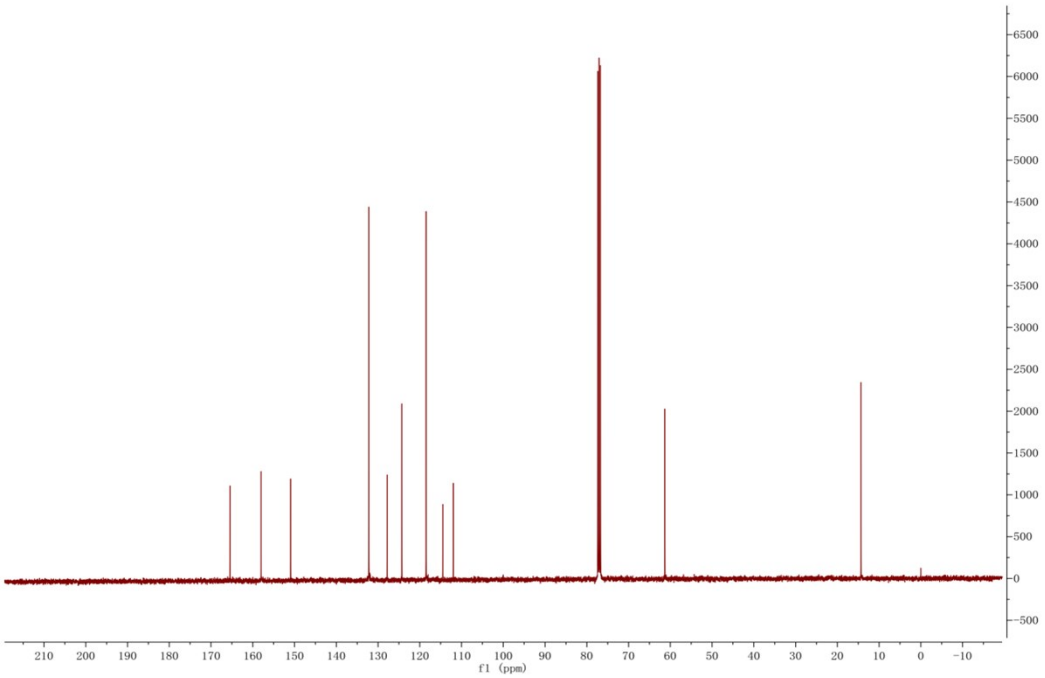

Fig. S2. ^{13}C NMR spectrum of **1** in $CDCl_3$.

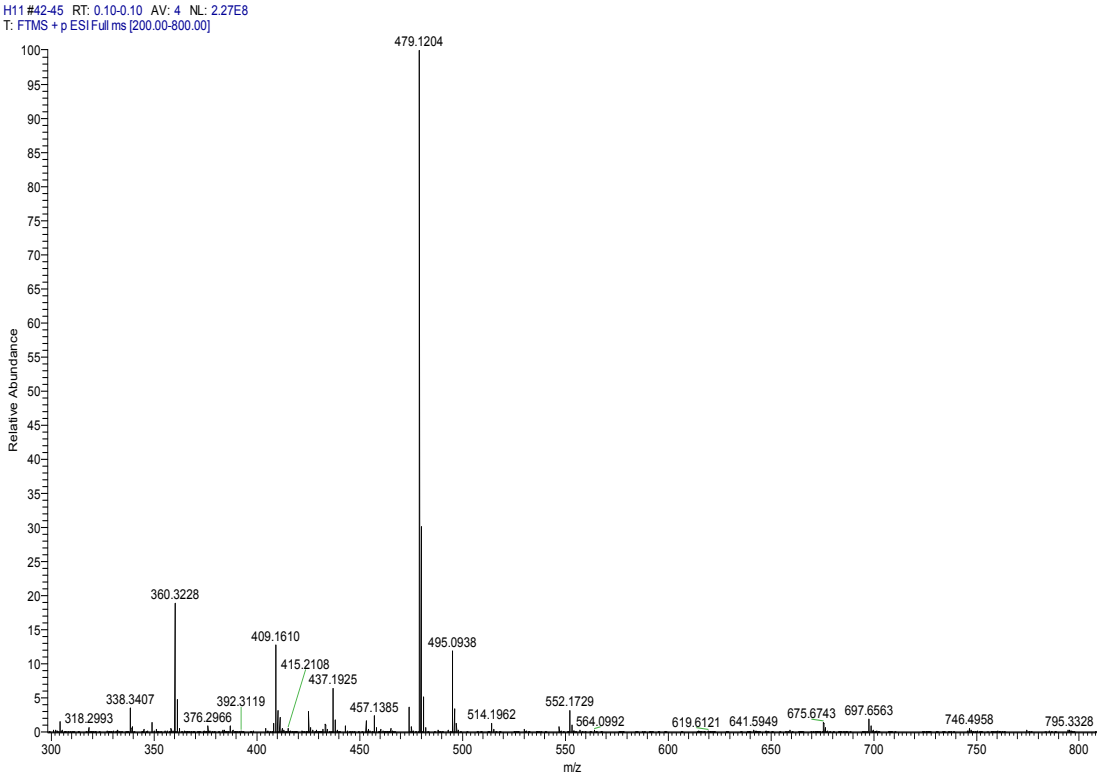

Fig. S3. HRMS spectrum of **1**.

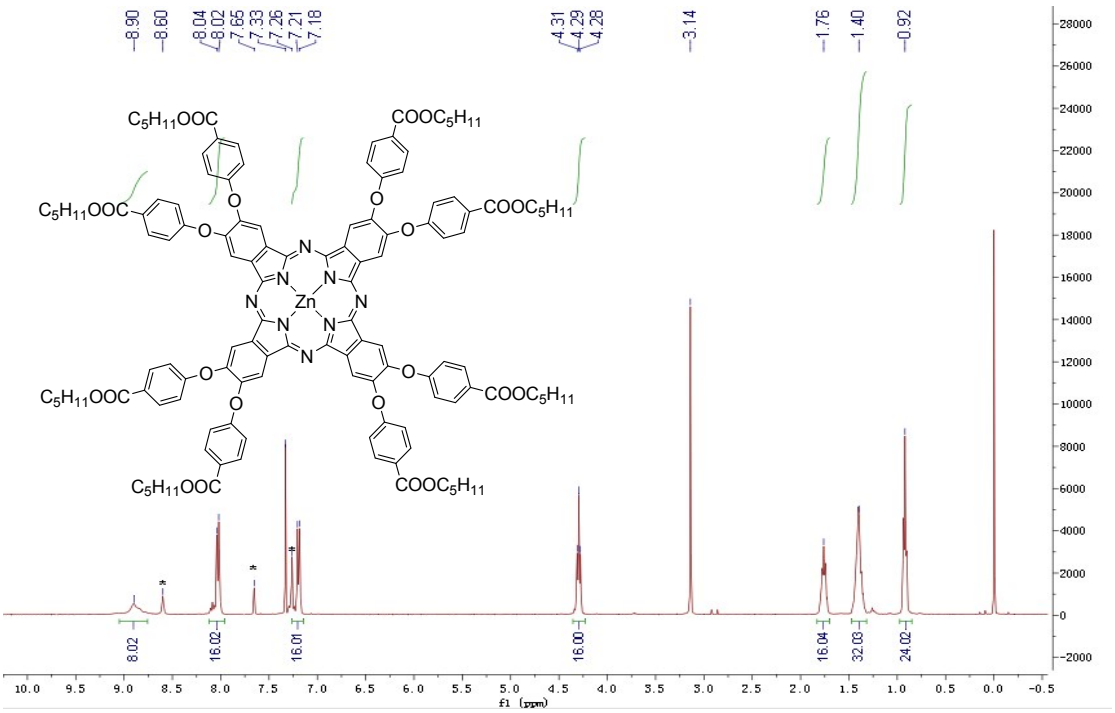

Fig. S4. ^{1}H NMR spectrum of **Pc1** in $CDCl_3$+ pyridine-d_5.

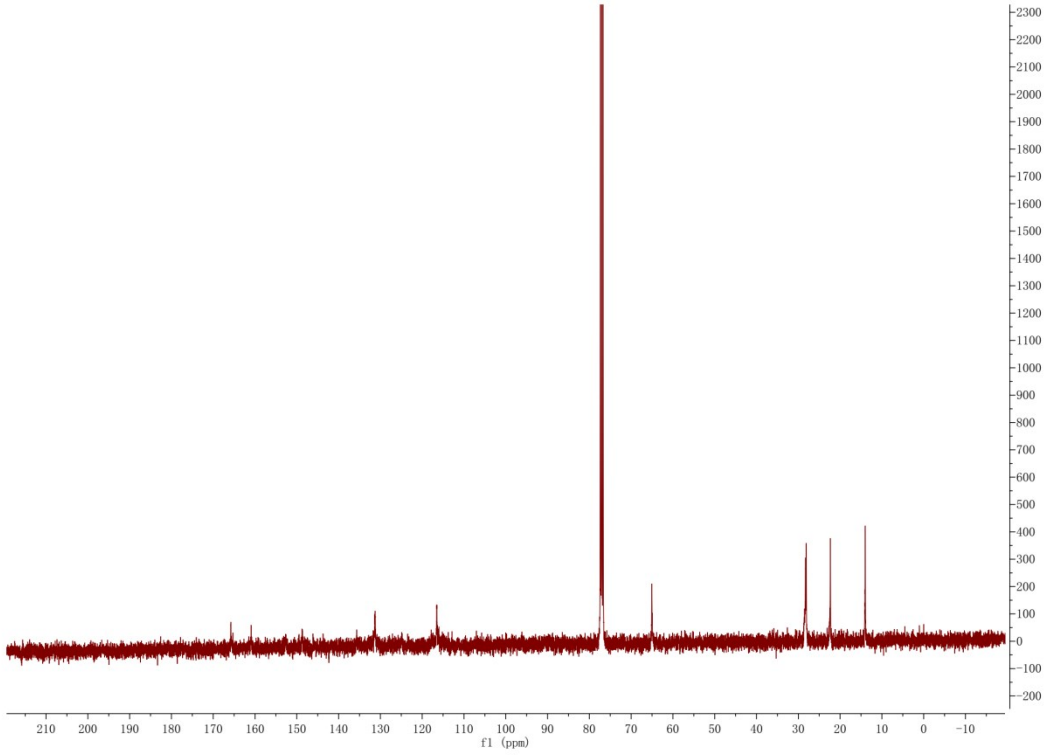

Fig. S5. ^{13}C NMR spectrum of **Pc1** in $CDCl_3$.

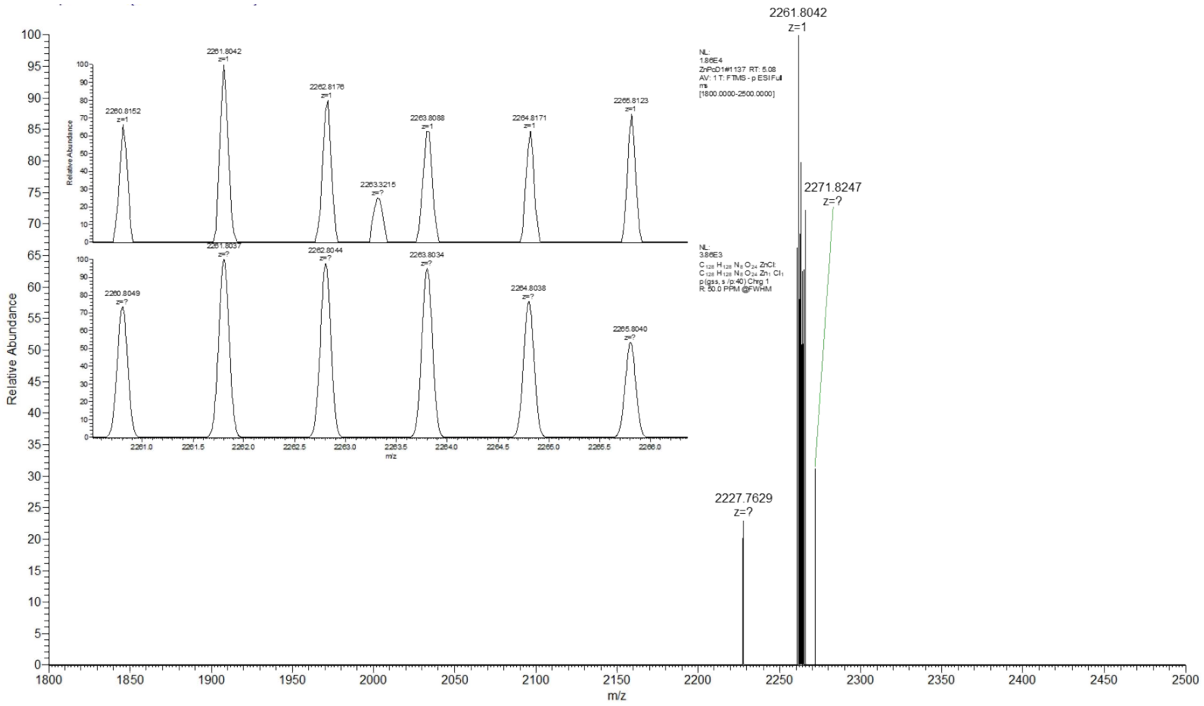

Fig. S6. HRMS spectrum of **Pc1**.

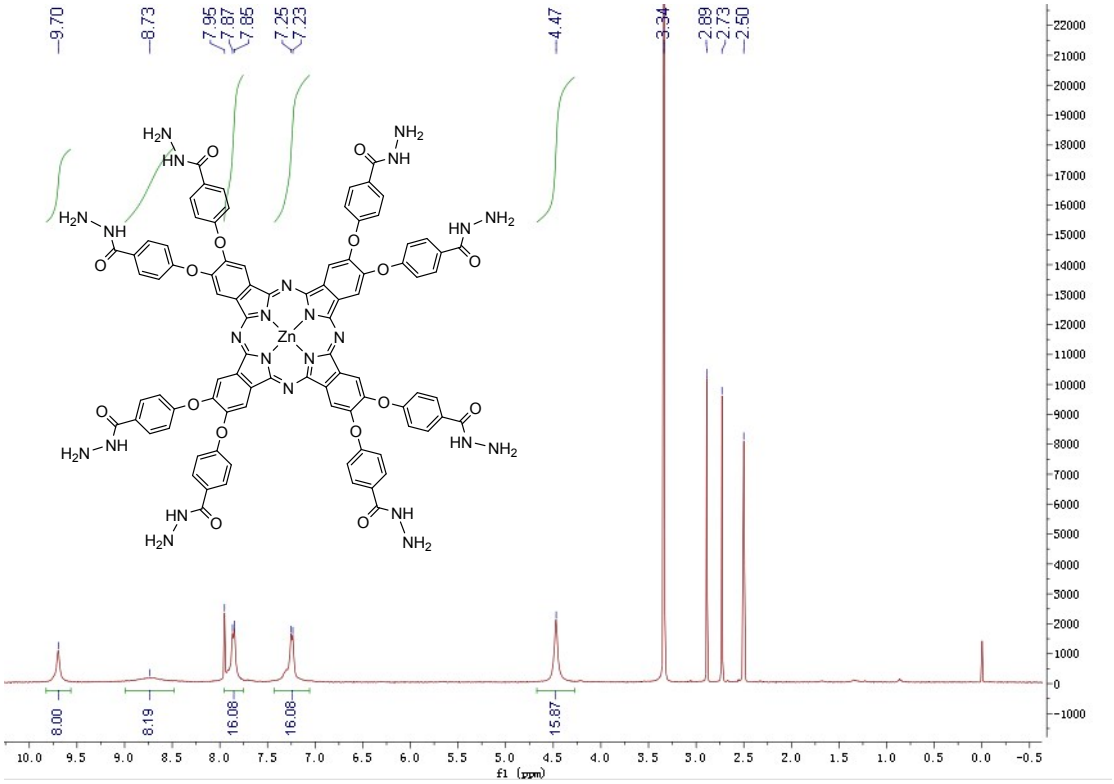

Fig. S7. ^{1}H NMR spectrum of **Pc2** in DMSO-d_6.

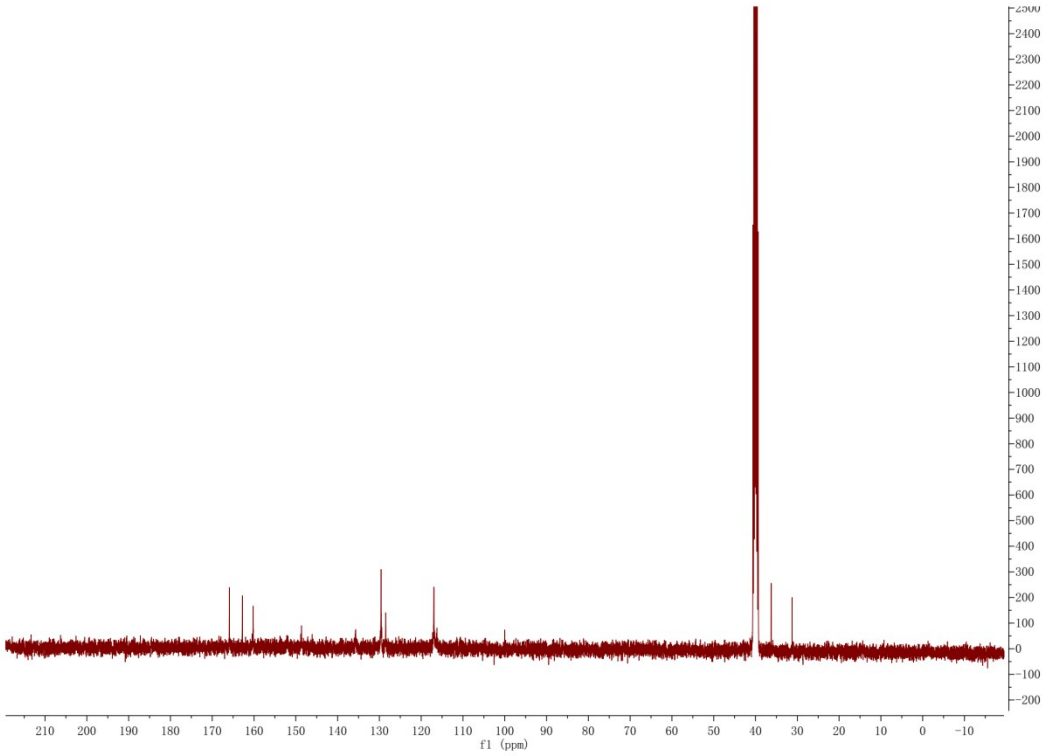

Fig. S8. ^{13}C NMR spectrum of **Pc2** in DMSO-d_6.

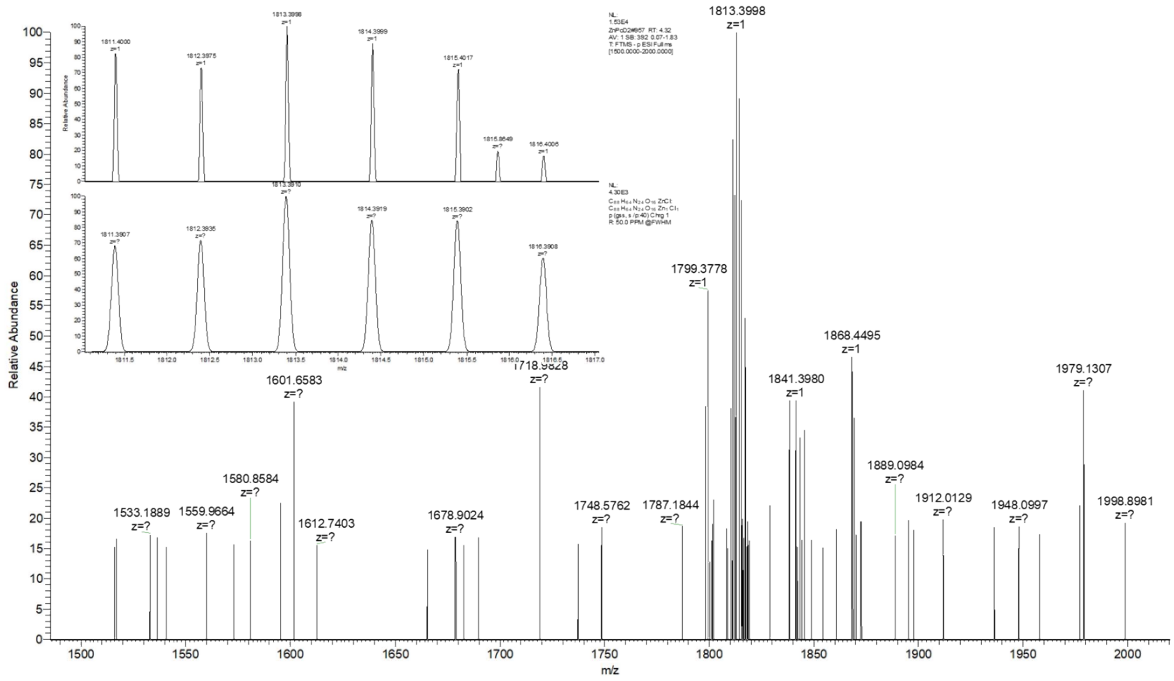

Fig. S9. HRMS spectrum of **Pc2**.

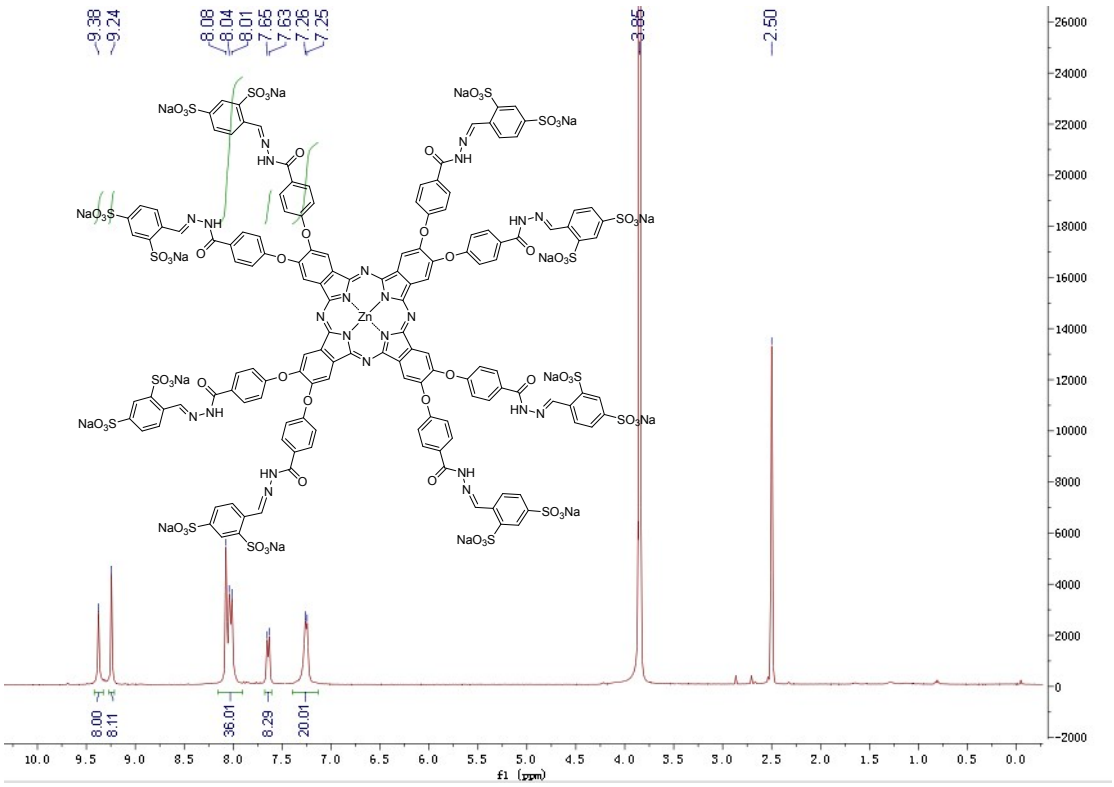

Fig. S10. ^{1}H NMR spectrum of **Pc3** (DMSO-d_6 + D_2O).

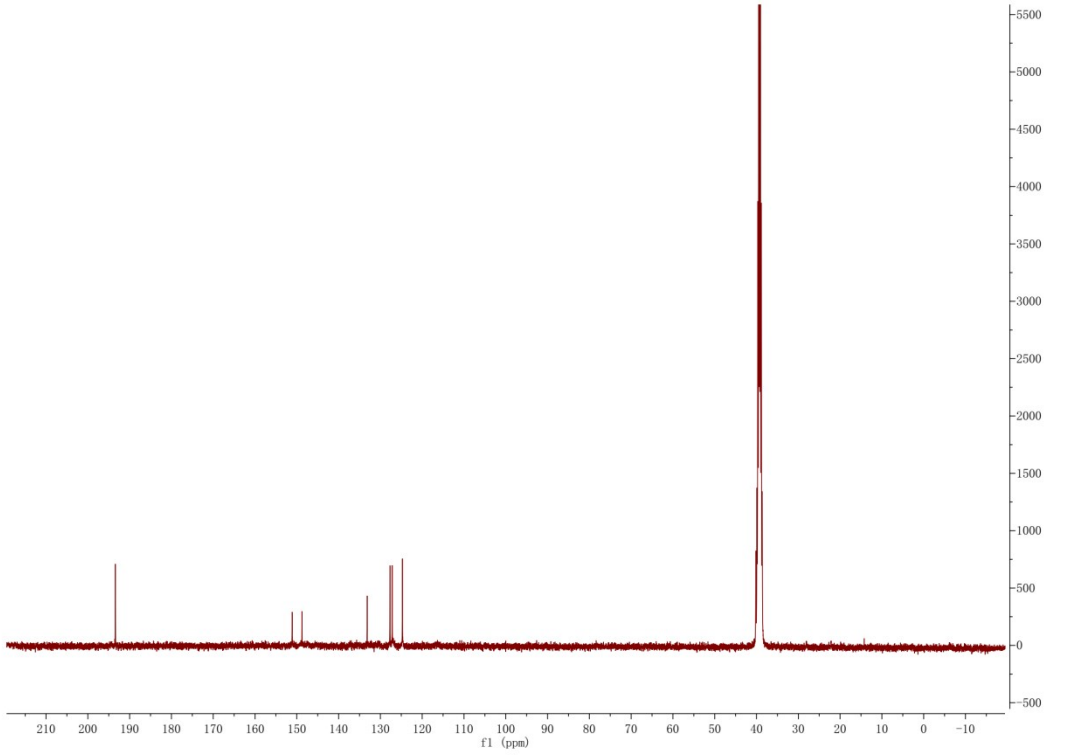

Fig. S11. ^{13}C NMR spectrum of **Pc3** in DMSO-d_6.

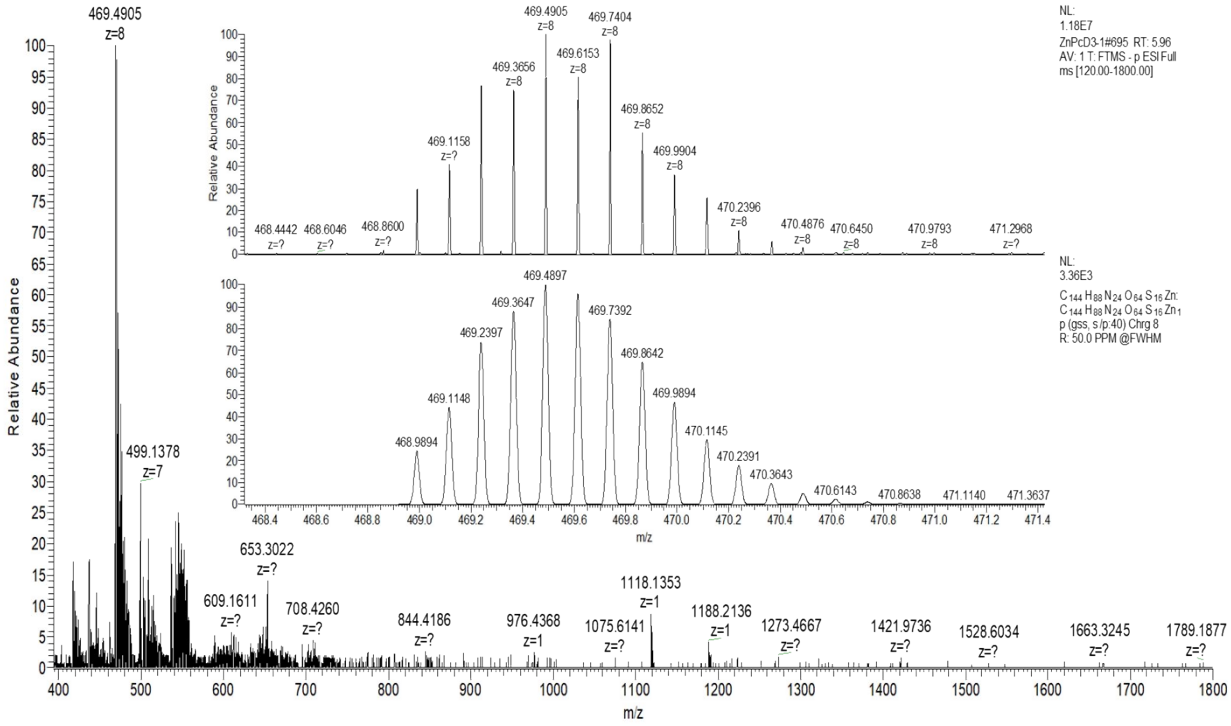

Fig. S12. HRMS spectrum of **Pc3**.

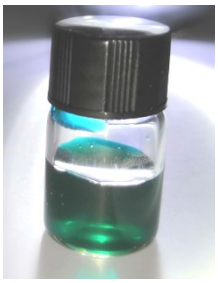

Fig. S13. Pc3 aqueous solution with a concentration of 8 mg mL^{-1}.

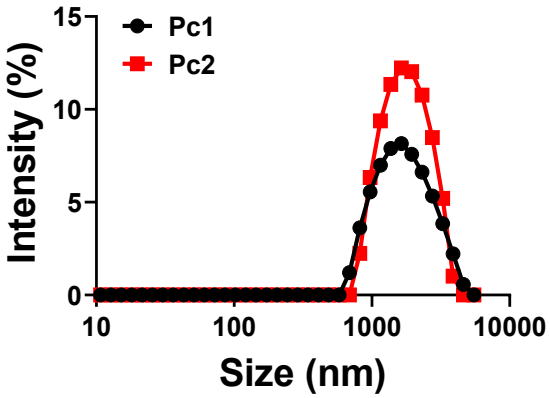

Fig. S14. Size distribution of **Pc1** and **Pc2** in H_2O detected by DLS (both at 5 μM, self-assembled for 12 h and stored in 4 °C).

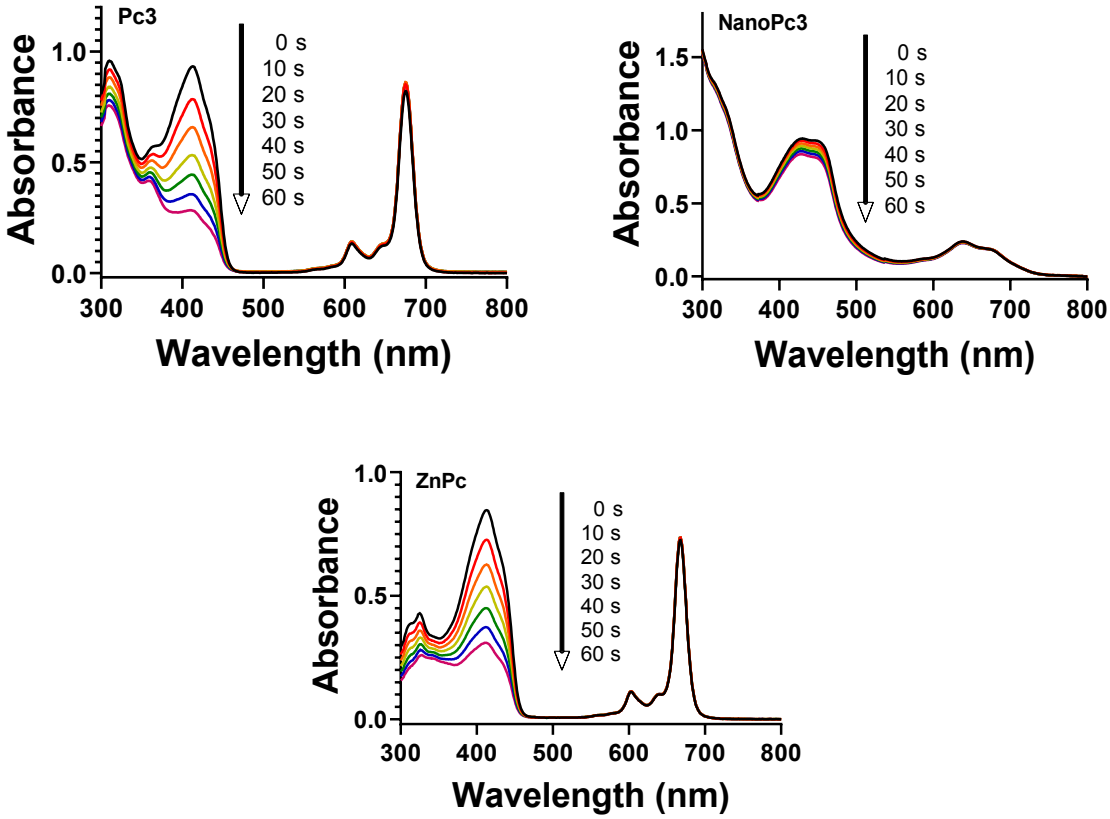

Fig. S15. $^1O_2$ generation kinetics of **Pc3** and ZnPc in DMF and **NanoPc3** in H_2O (5 μM) (n = 3). 1, 3-diphenylisobenzofuran (DPBF) was used as a probe. A_0 and A are absorbance of DPBF at initial time and different irradiation time points (λ > 610 nm), respectively.

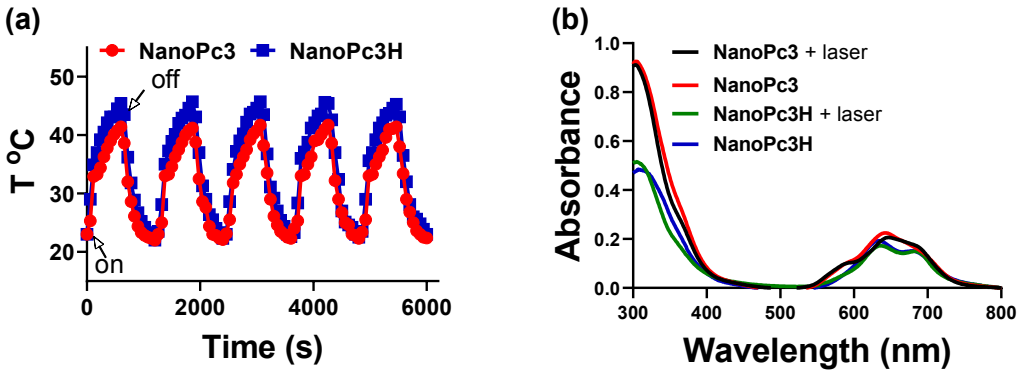

Fig. S16. (a) Temperature change curves of **NanoPc3** and **NanoPc3H** solutions (10 μM) in water over five cycles of on/off laser irradiation (730 nm, 0.52 W cm^{-2}). (b) Absorption spectra of **NanoPc3** and **NanoPc3H** solutions (10 μM) in water before and after 730 nm laser irradiation (0.52 W cm^{-2}, 1 h).

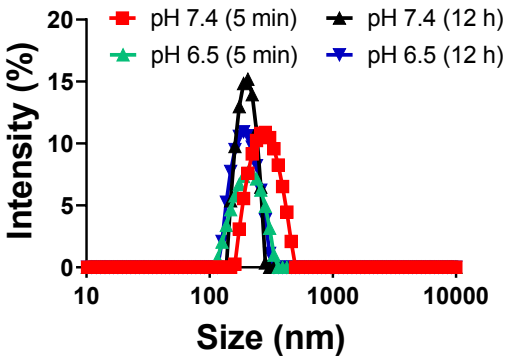

Fig. S17. Size distribution of **NanoPc3** in PBS at pH 7.4 and pH 6.5 at different time points, detected by DLS.

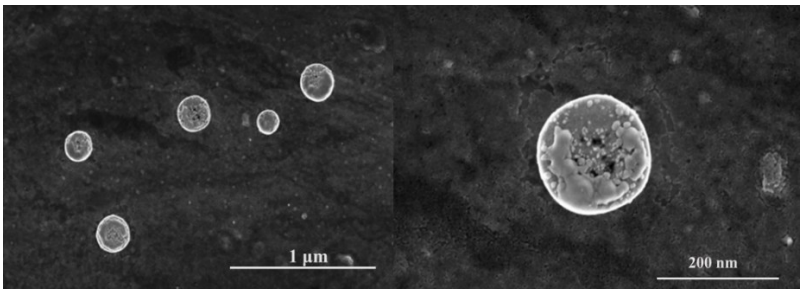

Fig. S18. TEM images of **NanoPc3H**.

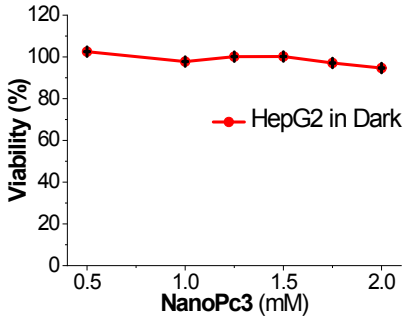

Fig. S19. Cytotoxicity of **NanoPc3** against HepG2 cells in the dark.

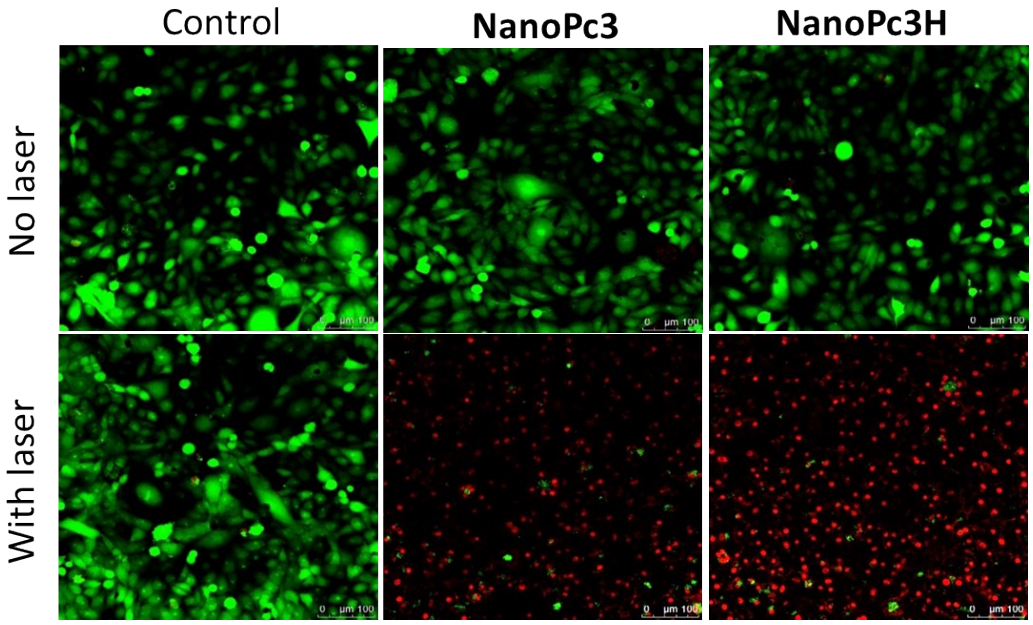

Fig. S20. Fluorescence images of HepG2 cells after incubation with NanoPc3 or NanoPc3H (both at 4 μM) for 2 h in the absence of presence of laser irradiation ((laser: 730 nm, 0.52 W cm^{-2}, 5 min), and then costained with Calcein-AM (green fluorescence) and propidium iodide (PI) (red fluorescence). Scale bar: 100 μM.

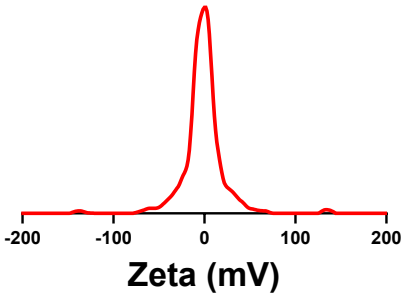

Fig. S21. Zeta potential of **NanoPc3** extracted from tumor tissues after intratumoral injection for 8 h.

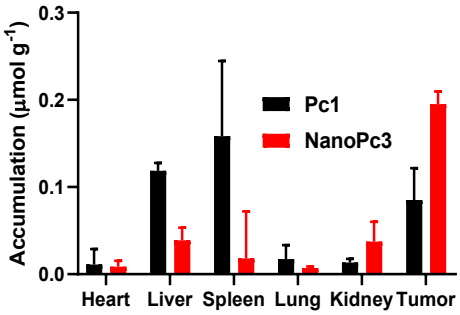

Fig. S22. Tissue distribution of **NanoPc3** and **Pc1** in the mice, measured through an *ex vivo* extraction method at 8 h post-injection. (n = 3)

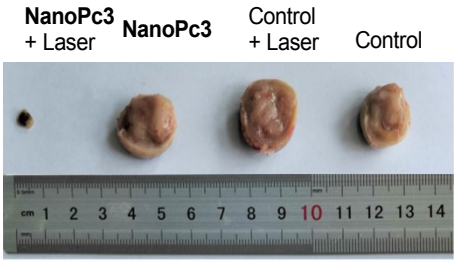

Fig. S23. Representative tumor images excised from the mice at 14 day post-treatments. (n = 5)